

Surinamite: A high-temperature metamorphic beryllosilicate from Lewisian sapphirine-bearing kyanite-orthopyroxene-quartz-potassium feldspar gneiss at South Harris, N.W. Scotland

SOTARO BABA,^{1,*} EDWARD S. GREW,² CHARLES K. SHEARER,³ AND JOHN W. SHERATON^{4,†}

¹Department of Geosciences, Osaka City University, Sugimoto 3-3-138, Osaka, 558-8585 Japan

²Department of Geological Sciences, University of Maine, 5790 Bryand Center, Orono, Maine 04469-5790, U.S.A.

³Institute of Meteoritics, University of New Mexico, Albuquerque, New Mexico 87131, U.S.A.

⁴Geology Department, Australian National University, Canberra, ACT 0200, Australia

ABSTRACT

The sapphirine-like mineral surinamite, $(\text{Mg}, \text{Fe}^{2+})_3(\text{Al}, \text{Fe}^{3+})_3\text{O}[\text{AlBeSi}_3\text{O}_{15}]$, occurs at South Harris as tiny grains enclosed in kyanite or as tabular grains up to 1 mm long mostly surrounded by Si-rich cordierite. A few surinamite grains enclose orthopyroxene, sillimanite, and Si-rich sapphirine. Ion microprobe analyses gave 3.52 to 3.81 wt% BeO (0.766 to 0.824 Be atoms per formula unit) and 2 to 13 ppm B in surinamite. Excess Si suggests the presence of significant BeO in cordierite and sapphirine. Given the anti-clockwise *P-T*-time path inferred for the South Harris rock, we suggest that surinamite formed at first by the continuous reaction BeSiAl_2 (in sapphirine) + sillimanite + orthopyroxene \rightarrow surinamite + quartz and, subsequently, by the discontinuous reaction Be-depleted sapphirine + quartz \rightarrow surinamite + orthopyroxene + kyanite with increase of *P* to >12 kbar at 850–900 °C. Surinamite reacted with orthopyroxene, kyanite, and quartz to form beryllian cordierite during subsequent decrease in *P* and *T*.

The high-silica content and peraluminous composition of the surinamite-bearing gneiss are consistent with a metasedimentary origin; this rock is markedly depleted in Th (0.13 ppm), U (0.11 ppm), Y (0.94 ppm), and rare-earth elements (e.g., Ce 7.7 ppm). Its bulk Be content (9 ppm) is not excessive. The appearance of a discrete Be phase in Be-poor rocks could be due to the absence of potential carriers of Be, namely muscovite and primary cordierite, at high *T* and low-water activity. Moreover, surinamite is indicative of a distinctive metamorphic history in which high-temperature rocks recrystallized at higher pressures or are isobarically cooled, and, consequently, scarcity of Be in metamorphic systems is not the only factor controlling surinamite formation.

INTRODUCTION

The sapphirine-like, beryllosilicate mineral surinamite, $(\text{Mg}, \text{Fe}^{2+})_3\text{Al}_4\text{BeSi}_3\text{O}_{16}$ (Moore and Araki 1983), was originally discovered in the Bakhuis Mountains, Surinam (de Roever et al. 1976), and subsequently reported at six other localities (Table 1). A seventh report from the Vijayanagaram District in the Eastern Ghats belt, India (Ramesh Kumar et al. 1995) needs confirmation. Surinamite is found in paragneisses or pegmatites that have been metamorphosed under upper amphibolite- and granulite-facies conditions at 8–12 kbar, 800–950 °C. De Roever and Vrána (1985) and Grew (1998) have suggested that surinamite formed from the breakdown of beryllian cordierite or another beryllian Al-rich mineral during a superimposed metamorphic event at relatively high-temperatures and pressures. Hölscher et al. (1986) reported that synthetic surinamite was stable from 4 kbar to at least 20 kbar and at *T* > 640 °C in

the MgO-BeO-SiO₂-Al₂O₃-H₂O system; optimal conditions for synthesis from a seeded gel were found to be near 840 °C at 9–13 kbar. The experiments confirm that surinamite is a high-temperature mineral requiring moderate pressure to form.

We present here a detailed chemical and petrologic study of surinamite that Baba (1998b, 1999) discovered in an orthopyroxene-kyanite gneiss (no. 96820-spl, Opx-Ky granulite) in the Benn Obbe Quartzite of the granulite-facies Leverburgh belt (Fig. 1). This gneiss is one of two paragneisses containing traces of sapphirine, another mineral only recently found in the Lewisian (Baba 1998b). Baba (1998a, 1999) recognized an anti-clockwise *P-T* path involving four metamorphic stages (M1-M4) for the Leverburgh belt. M1 resulted from the thermal action of the South Harris Igneous Complex ca. 2.18–1.84 Ma (Cliff et al. 1983); the most recent estimates for conditions of thermal metamorphism are 9–11 kbar and 900–980 °C (Baba 1998b, 1999). Baba (1998b, 1999) interpreted the textural relations of sapphirine in the orthopyroxene-kyanite gneiss to indicate that the sapphirine + quartz assemblage had been stable during M1. Pressure during the regional M2 granulite-facies event increased to 13–14 kbar while temperatures remained high at 850–900 °C, so that Opx was stabilized with Ky (*P* > 12 kbar, Baba 1999; cf., Wood 1975, 1977). Ret-

* Present address: National Institute of Polar Research, Kaga 1-9-10, Itabashi-ku, Tokyo 173-8515, Japan. E-mail: baba@nipr.ac.jp

† Present address: Stoneacre, Bream Road, St. Briavels, Lydney, Glos GL15 6TL, U.K.

TABLE 1. World surinamite localities

Locality	Host rock	Associated minerals	P-T conditions	Possible reaction
1. Bakhuis Mtns, Surinam	Mylonitic meso-perthite gneiss	Qtz, Kfs, Pl, Bt, Sil, Ky, Spl	Granulite-facies	$\text{Crd} \rightarrow \text{Sur} + \text{Al}_2\text{SiO}_5 + \text{Qtz}$
2. Strangways Range, central Australia	Aluminous granulite	Included in Crd. Also Qtz, Spl, Spr, Phl, Opx, Sil, opaque oxide	$T < 900\text{-}950\text{ }^\circ\text{C}$ $P \sim 8\text{-}9\text{ kbar}$	
3. "Christmas Point", Casey Bay, Antarctica	Meta-pegmatite	Qtz, Kfs, Sil, Spr, khmaralite*, wagnerite, Grt, Opx, Bt, Hem, Mgt, Spl, musgravite, Crn; 2 nd Crd, And, Ky	$T \geq 820\text{ }^\circ\text{C}$, $P \geq 10\text{ kbar}$	Khmaralite or beryllian Spr + Qtz \rightarrow Sur + Grt + Sil
4. "Zircon Point", Casey Bay, Antarctica	Meta-pegmatite	Qtz, Kfs, Pl, Sil, Ky, khmaralite*, musgravite, dumortierite, Cb, Grt, Bt, Rt	$T \geq 820\text{ }^\circ\text{C}$, $P \geq 10\text{ kbar}$	
5. Mount Pardoe, Amundsen Bay, Antarctica	Meta-pegmatite	Enclosed in 2 nd Crd with Sil, Bt. Also Qtz, Kfs, wagnerite, Grt, Opx, And, Ky	$T \geq 820\text{ }^\circ\text{C}$, $P \geq 10\text{ kbar}$	
6. Chimwala area, Zambia	Cordierite granulite	Qtz, Kfs, Pl, Bt, Ky, Grt, Mgt. Crd and a Sil-like mineral are completely replaced	Amphibolite, transitional to granulite facies	$\text{Crd} + \text{Kfs} + \text{H}_2\text{O} \rightarrow \text{Sur} + \text{Ky} + \text{Bt} + \text{albite}$
7. South Harris, Scotland, U.K.	gneiss	Qtz, Kfs, Spr, Opx, Ky, Sil, 2 nd Crd	$T = 850\text{ - }900\text{ }^\circ\text{C}$, $P > 12\text{ kbar}$: M2 stage	See text

Note: Source of information on surinamite localities: 1 = de Roever (1973), de Roever et al. (1976); 2 = Woodford and Wilson (1976), Goscombe (1992); 3, 4, 5 = Grew (1981, 1998); Grew et al. (2000); 6 = Vavra and Vrána (1972), de Roever and Vrána (1985); 7 = this paper, Baba (1999). *Khmaralite is a Be-rich member of the sapphirine group (Barbier et al. 1999). Abbreviations: And = andalusite, Bt = biotite, Cb = chrysoberyl, Crd = cordierite, Crn = corundum, Grt = garnet, Hem = hematite, Ilm = ilmenite, Kfs = alkali feldspar, including mesoperthite, Ky = kyanite, Mgt = magnetite, Opx = orthopyroxene, Phl = phlogopite, Pl = plagioclase, Qtz = quartz, Rt = rutile, Sil = sillimanite, Spl = spinel, Spr = sapphirine.

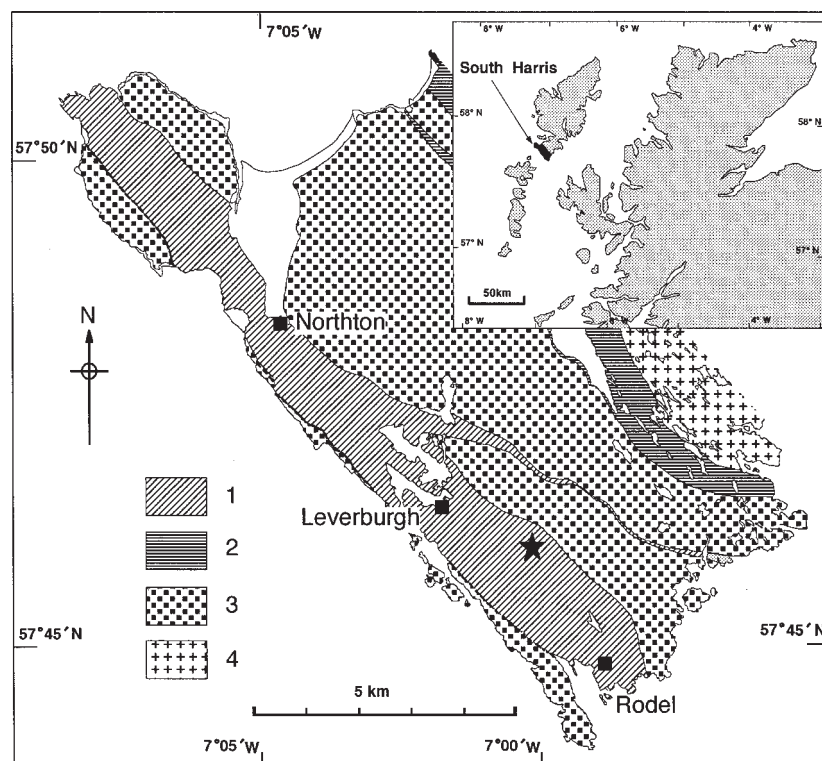


FIGURE 1. Map of a portion of Lewisian Complex in South Harris showing localities for surinamite-bearing gneiss. 1 = Leverburgh belt; 2 = Langavat belt; 3 = South Harris Igneous Complex; 4 = Migmatitic acid gneiss with granite and pegmatite. The star marks the locality of the surinamite-bearing gneiss.

rograde events involved decompression under relatively dry conditions as evidenced by coronas and symplectites (M3), which was followed by fluid infiltration accompanied by development of a foliation and alteration to hydrous minerals (M4, Baba 1998a). These studies provide a well-characterized framework for understanding how surinamite forms in a metamorphic environment.

DESCRIPTION OF THE SURINAMITE-BEARING GNEISS

The surinamite-bearing gneiss is found in a small outcrop about 0.5 km south of Roineabhal summit. This gneiss occurs as a thin layer not exceeding 1 m in thickness within orthopyroxene-bearing quartzofeldspathic gneiss; it is relatively rich in potassium feldspar compared to the orthopyroxene-bearing gneiss. Thin Al_2SiO_5 -bearing layers and a garnet-bearing layer are also found in the orthopyroxene-bearing gneiss. The surinamite-bearing gneiss consists dominantly of medium-grained (0.5 to 1 mm) quartz and pale-pink potassium feldspar. Plagioclase, orthopyroxene, biotite, cordierite, kyanite, and sillimanite are subordinate, whereas surinamite, zircon, apatite, garnet, and sapphirine are present in trace amounts. In places, grains of orthopyroxene, quartz, and potassium feldspar are ellipsoidal in strongly sheared domains. Plagioclase is much subordinate to potassium feldspar and a few grains are myrmekitic. Orthopyroxene occurs both as porphyroblasts up to 20 mm across and in intergrowths with kyanite and sillimanite. Both the relatively dark and pale varieties of biotite are secondary. Pale biotite generally forms aggregates along margins of orthopyroxene grains and randomly oriented flakes in cordierite, whereas dark biotite is concentrated in aggregates flattened parallel to the quartz and potassium feldspar foliation. Flakes reach 0.8 mm, but most are finer (0.1–0.3 mm). Most kyanite prisms and a few secondary sillimanite prisms have a preferred orientation together with secondary biotite, quartz, and potassium feldspar. Cordierite forms coronas around orthopyroxene-kyanite/sillimanite intergrowths, kyanite, sillimanite, and surinamite. Muscovite is finer grained than biotite, and occurs as flakes in pinitized cordierite and rarely replacing biotite.

Surinamite occurs in two distinct forms: (1) as tiny grains enclosed in kyanite or at the margins of kyanite grains, and (2) as tabular grains up to 1 mm long surrounded by cordierite coronas (Fig. 2a), rarely mantled by sillimanite, which in turn are surrounded by quartz in the matrix. In places, surinamite is in direct contact with quartz with no intervening cordierite. Tabular surinamite locally encloses rounded grains of sillimanite, orthopyroxene (Fig. 2a), and irregular shaped sapphirine (Fig. 2b). Potassium feldspar encloses surinamite grains without formation of cordierite coronas. The South Harris surinamite is pleochroic in pale purple (X), pale yellow green (Y), and blue green (Z).

Chemistry of the surinamite and associated minerals

Constituents other than Be and B were analyzed in surinamite and associated minerals by wavelength-dispersive methods on a JEOL 8800 Superprobe at Ehime University using 15 kV accelerating voltage and 5 nA beam current and a SHIMAZU 8705 electron microprobe at Osaka City Univer-

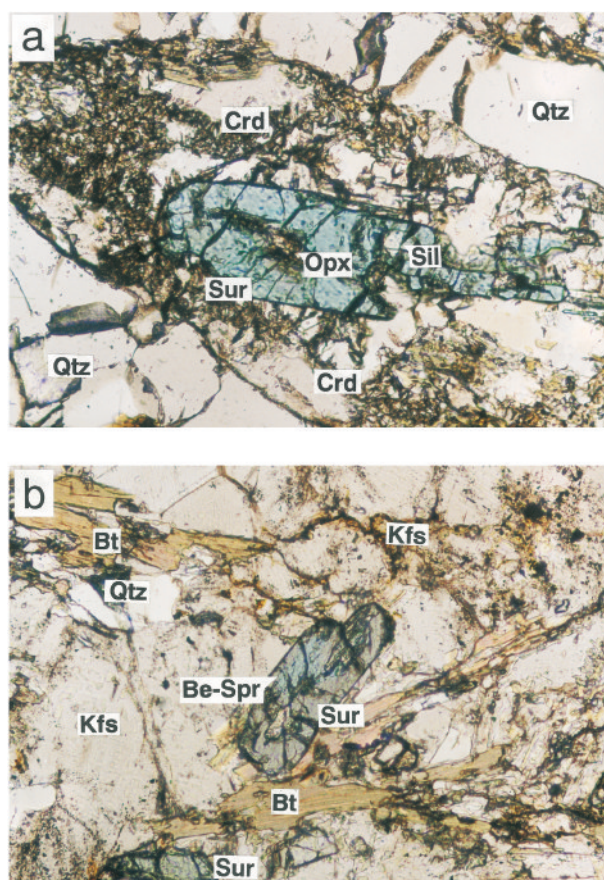


FIGURE 2. Photomicrographs of surinamite in specimen no. 96820-sp1 (a) Orthopyroxene (Opx) and sillimanite (Sil) are enclosed by surinamite (Sur), which was partially replaced by corona of secondary cordierite (Crd); these minerals are surrounded by quartz matrix (Qtz). (b) Surinamite encloses sapphirine, presumed to be beryllian (Be-Spr). Surinamite is surrounded by potassium feldspar (Kfs) and secondary biotite (Bt), cordierite, and a small amount of quartz. Note the absence of a cordierite corona between surinamite and potassium feldspar. Width of the photomicrographs is 1.2 mm.

sity using 15 kV accelerating voltage and 4 nA beam current. Data were reduced by ZAF and Bence-Albee methods, respectively. The following minerals, which were purchased from JEOL, Ltd., were used for standards: wollastonite (Ca, Si), quartz (Si at Ehime University), pyrophanite (Mn, Ti), corundum (Al), fayalite (Fe), periclase (Mg), albite (Na), and potassium feldspar (K). All of analyses were counted for 10 seconds with 5 seconds for background.

Be and B were analyzed by secondary ion mass spectrometry using a Cameca ims 4f ion microprobe operated on the University of New Mexico (UNM) campus by a UNM and Sandia National Laboratories consortium. These elements were analyzed under the following conditions: $^{16}O^-$ primary beam accelerated through 12.5 kV, 10 nA primary beam current, 25 micrometers beam diameter, sample voltage offset of -50 V, a mass resolution of approximately 320, and a 150 micrometers secondary ion image field with a 33 micrometers field aperture inserted. Prior to analysis, each analytical spot was prepared

by rastering the ion beam over an area of 125×125 micrometers. The area to be analyzed on each grain was checked for compositional homogeneity and impurities by ion imaging of Be, Si, Al, Mg, Ca, Na, and K. Consequently, we consider it unlikely that contamination from inclusions or adjacent phases affected the Be content of surinamite. The following individual counting times were used in each cycle: background at mass 6.5 (2 seconds), ^9Be (3 seconds), ^{11}B (4 seconds) and ^{30}Si (2 seconds) were used in each cycle. Each spot analysis involved 20 counting cycles; rare, obviously aberrant individual cycles were excluded from the average. These counting times resulted in internal precision for Be and B of better than 3%. Calibration curves for Be and B (trace element / $^{30}\text{Si} \times \text{wt}\% \text{SiO}_2$ vs. trace element concentration) were defined by "Christmas Point" surinamite (no. 2292C) for Be and prismatic and grandierite (no. BM1940,39) for B.

Surinamite

To provide a context for our discussion of the South Harris surinamite, we will briefly review available compositional data on this little known mineral. Fourteen analyses have been published (including Table 2, but excluding the analyses reported by Ramesh Kumar et al. 1995); these data are plotted in Figure 3. De Roever et al. (1981) proposed a model formula $(\text{Mg}_{2.25}\text{Fe}_{0.75})(\text{Al}_{3.75}\text{Fe}_{0.25})(\text{BeSi}_3\text{O}_{16})$ for the type surinamite, which Moore and Araki (1983) refined to approximately $^{\text{VI}}(\text{Mg,Fe})_3^{\text{VI}}\text{Al}_3^{\text{IV}}(\text{AlBeSi}_3\text{O}_{16})$ from a study of the crystal structure of a surinamite from "Christmas Point," Enderby Land, Antarctica (no. 2292C) (Grew 1981). The tetrahedral sites are highly ordered. J. Barbier (personal communication), who is presently carrying out a new crystal-structure refinement of another crystal from this specimen, has confirmed that the composition of the highly ordered tetrahedra is close to the ideal $\text{AlBeSi}_3\text{O}_{15}$. There is considerable Mg-Fe and Al-Fe exchange on the octahedral sites, but negligible Mg-Al exchange. If only Fe^{2+} replaces Mg and only Fe^{3+} replaces Al, the formula can be written as $(\text{Mg,Fe}^{2+})_3(\text{Al,Fe}^{3+})_3\text{O}[\text{AlBeSi}_3\text{O}_{15}]$.

No analysis of surinamite has included measurement of Fe valence state. The analyses have been normalized to 11 cations and 16 O atoms (to 10 cations and 15 O atoms in the absence of a Be determination) for calculating $\text{Fe}^{3+}/\text{Fe}^{2+}$ ratio and plotting in Figure 3. This normalization procedure introduces alignment of the plotted points, particularly for analyses in which an ideal Be content has been assumed ("other" and "South Harris Be = 1" in Figs. 3a and 3b). Calculated values of $\text{Fe}^{3+}/\text{Fe}^{2+}$ range from 0 to 0.54. The high $\text{Fe}^{3+}/\text{Fe}^{2+}$ contents (0.39–0.42) of "Christmas Point" surinamite (no. 2292C) are consistent with the crystal structure refinement (Barbier personal communication) and with the presence of hematite in the surinamite-bearing pegmatite at "Christmas Point". Overall, deviations from the ideal formula $(\text{Mg,Fe}^{2+},\text{Ca})_3(\text{Al,Fe}^{3+},\text{Cr})_3\text{O}[\text{AlBeSi}_3\text{O}_{15}]$ appear to follow the $\text{Al}_2(\text{MgSi})_{-1}$ (Tschermaks) and MgBe_{-1} substitutions (Fig. 3).

The composition of the South Harris surinamite differs from those of other analyzed occurrences in being richer in Si (average Si = 3.036 apfu) and total divalent cations except Be (average $\text{Fe}^{2+} + \text{Mn} + \text{Mg} + \text{Ca} = 3.171$ apfu), but poorer in Be, which ranges from 3.52 to 3.81 wt% BeO, i.e., from 0.766 to

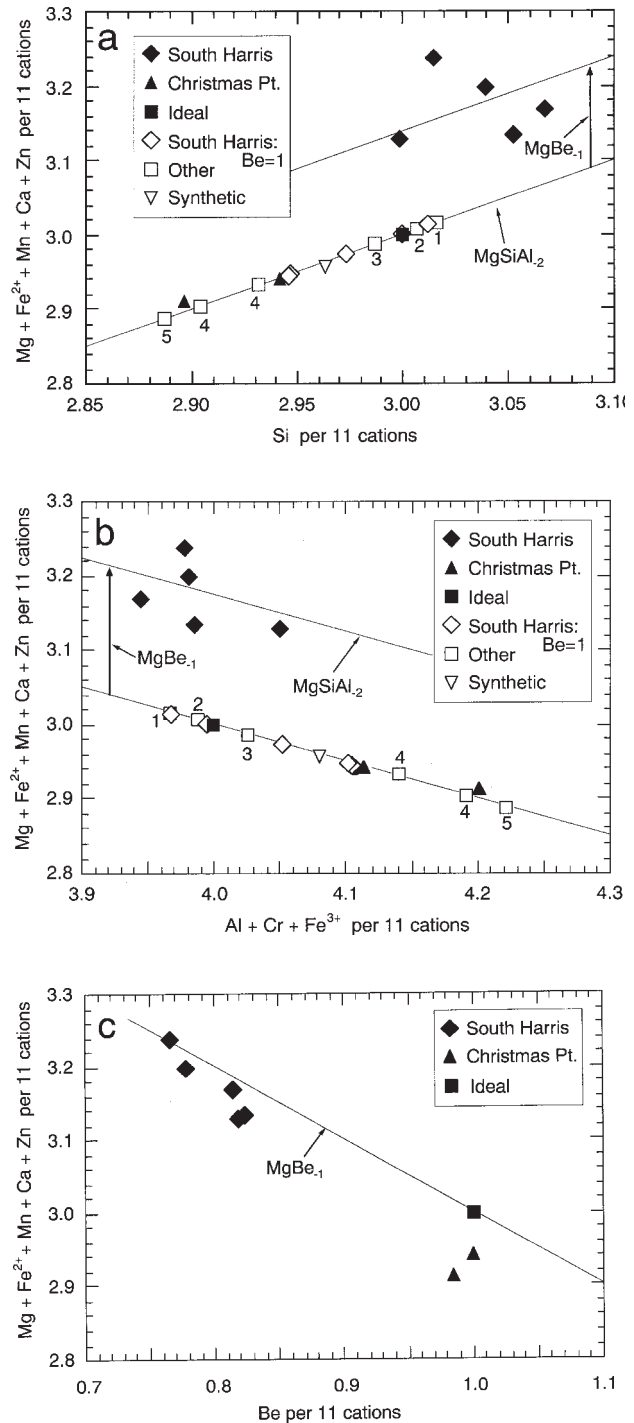


FIGURE 3. Compositional plots for surinamite. Sources of data for analyses including a Be determination (Filled symbols): South Harris (this paper); "Christmas Point" (Grew 1981 and J. Barbier unpublished data). Sources of data for analyses lacking a Be determination (unfilled symbols): Other 1. Bakhuis Mtns. (de Roever et al. 1976); 2. Strangways Range (Woodford and Wilson 1976); 3. Chimwala area (de Roever and Vrána 1985); 4. "Zircon Pt." Casey Bay (Grew 1981); 5. "Christmas Pt." Casey Bay (Grew 1981); synthetic (Hölscher et al. 1986).

TABLE 2. Representative analyses of surinamite in sample no. 96820-sp1

Grain. no. <i>n</i>	no.1 7	d14-1 2	d14-2 2	d14-3 2	no.3 4
Electron microprobe wt%					
SiO ₂	33.29	33.94	33.86	33.04	33.91
TiO ₂	0.04	0.08	0.02	0.03	0.05
Al ₂ O ₃	37.23	37.03	37.53	37.83	37.54
Cr ₂ O ₃	0.06	0.00	0.14	0.05	0.04
Fe ₂ O ₃	0.00	0.00	0.00	0.00	0.00
FeO	5.50	5.69	5.25	5.91	5.53
MnO	0.16	0.07	0.17	0.08	0.18
MgO	20.68	20.23	20.73	19.67	20.02
CaO	0.14	0.05	0.17	0.11	0.15
Na ₂ O	0.01	0.01	0.01	0.01	0.01
K ₂ O	—	—	—	—	—
ZnO	0.00	0.00	0.00	0.00	0.01
Ion microprobe wt%					
BeO	3.52	3.75	3.61	3.76	3.81
B ₂ O ₃	0.002	0.001	0.004	0.003	0.001
Total	100.63	100.85	101.49	100.49	101.25
Structural formulae based on 11 cations					
O	16.007	16.045	16.031	16.025	16.048
Si	3.015	3.068	3.040	2.999	3.053
Be	0.766	0.814	0.778	0.820	0.824
B	0.000	0.000	0.001	0.000	0.000
Ti	0.003	0.005	0.001	0.002	0.003
Al	3.975	3.945	3.971	4.047	3.983
Cr	0.004	0.000	0.010	0.004	0.003
Fe ³⁺	—	—	—	—	—
Fe ²⁺	0.417	0.430	0.394	0.449	0.416
Mn	0.012	0.005	0.013	0.006	0.014
Mg	2.793	2.726	2.774	2.661	2.687
Ca	0.014	0.005	0.016	0.011	0.014
Na	0.002	0.002	0.002	0.002	0.002
K	—	—	—	—	—
Zn	0.000	0.000	0.000	0.000	0.001
X _{Mg}	0.870	0.864	0.876	0.856	0.866

Note: *n* = number of analyses averaged. X_{Mg} = Mg/(Mg + Fe²⁺). Fe³⁺ is calculated from charge balance.

0.824 Be per formula unit of 11 cations (Table 2). The South Harris surinamite is also among the most magnesian, i.e., X_{Mg} = Mg/(Fe²⁺+Mg) = 0.86–0.88 compared with X_{Mg} = 0.75–0.87 in other surinamite. As oxygen totals calculated for 11 cations exceed 16 in the South Harris surinamite, we infer that Fe³⁺ content is negligible. Analyses that include the SIMS Be contents plot in a linear trend parallel to MgBe₋₁ (Fig. 3c). For example, if an ideal Be=1 apfu is assumed for the South Harris surinamite, a portion of the Fe is calculated to be Fe³⁺ and scatter in the points is eliminated (Figs. 3a and 3b). A coupled substitution ^{IV}Al → ^{IV}Be and ^{VI}Mg → ^{VI}Al, which sums to Mg → Be, could explain the apparent deficiency in Be and excess of the other divalent cations in the South Harris surinamite. The presence of Be-Al mixing on a tetrahedral site has been demonstrated in khmaralite (Barbier et al. 1999), as well as in cordierite (e.g., Armbruster 1986).

Sapphirine

Compositions of sapphirine enclosed in surinamite and kyanite (Table 3) are anomalous in their low analytical and cation totals, together with high Si and low Al contents relative to expected stoichiometry for sapphirine, (Mg,Fe²⁺)₇(Al,Fe³⁺)₁₈Si₃O₄₀ — (Mg,Fe²⁺)₈(Al,Fe³⁺)₁₆Si₄O₄₀. Compositions of sapphirine in thin sections lacking surinamite

from Opx-Ky gneiss have the expected stoichiometry (Baba 1999). We suggest that these anomalous features are due to ignoring Be incorporated in the sapphirine. Ion probe analyses of khmaralite and beryllian sapphirine from Enderby Land, Antarctica, and the Musgrave Ranges, Australia, show that Be is incorporated in sapphirine by the substitution BeSiAl₂, that is, beryllian sapphirine compositions lie approximately along the join Mg_{7.2}Al_{17.6}Si_{3.2}O₄₀—Mg_{7.2}Al_{14.4}Be_{1.6}Si_{4.8}O₄₀ (khmaralite), where Fe²⁺ is combined with Mg and Fe³⁺ with Al (Grew 1981; Barbier et al. 1999; Grew et al. 2000). If the amount of Be in the sapphirine is assumed to be 1.25 wt% BeO, equivalent to 0.7 Be apfu or 50% of the amount of Be in khmaralite, then analytical totals approach or exceed 100% (Table 2), cation totals approach or exceed 28 per 40 O atoms, and compositions plot in a linear array nearly parallel to that for ideal sapphirine (Fig. 4a). Two compositions plot close to Si = 4 apfu and Mg = 7.2, that is, about midway between the two limiting compositions cited above and consistent with the assumed Be content of 0.7 apfu. The variation among the South Harris sapphirine compositions is largely the result of the Tschermarks substitution MgSiAl₂, but scatter in the data suggests that Be content could vary slightly via the substitution BeSiAl₂. The

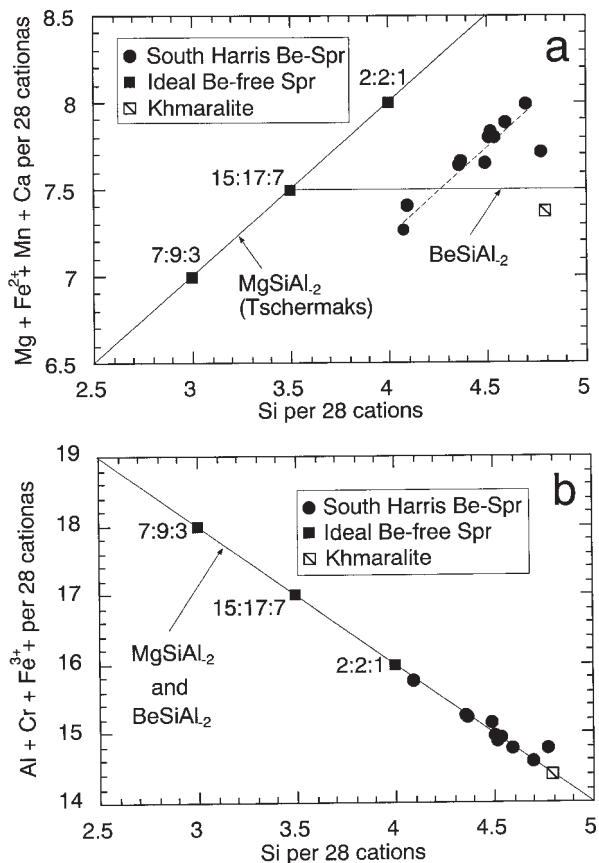


FIGURE 4. Compositional plots for Si-rich sapphirine from South Harris, which is presumed to be beryllian. Khmaralite composition is from Barbier et al. (1999). Ratios refer to proportions of (Mg, Fe, Mn, Ca)O, (Al, Fe³⁺, Cr)₂O₃, and SiO₂ in sapphirine, e.g., 2:2:1 corresponds to 2(Mg, Fe, Mn, Ca)O·2(Al, Fe³⁺, Cr)₂O₃·SiO₂.

trends for ideal and the South Harris sapphirines are nearly superimposed in a plot of Si vs. Al+Cr+Fe³⁺ because the variation between Si and trivalent cations is the same in MgSiAl₂ and BeSiAl₂ (Fig. 4b). The trend for the South Harris sapphirine implies that not all beryllian sapphirine compositions plot on a line between khmaralite and the Be-free composition (Mg, Fe)_{7.2}(Al, Fe)_{17.6}Si_{3.2}O₄₀ (Grew et al. 2000).

Cordierite

Although cordierite replacing orthopyroxene-kyanite intergrowths has the expected stoichiometry, cordierite replacing surinamite is distinctive in its high Si and low Al contents as well as in containing 0.54 to 0.56 wt% Na₂O (Table 4). A portion of the Na present could have been incorporated with Be by virtue of the substitution Na + Be → □ + Al (e.g., Černý and Povondra 1966). If all the Na, K, and Ca are assumed to be associated with Be, then the maximum possible amount of Be would be 0.12 Be pfu, but this amount still accounts for only part of the deficiency in Al, and does not explain the excess Si. It is possible that additional Be is incorporated by the substitution BeSiAl₂, which has been reported in synthetic solid solutions between cordierite and the cordierite-like phase Mg₂[Al₂BeSi₆O₁₈] that is isostructural with beryl (Hölscher and Schreyer 1989). Assuming the presence of 1 wt% BeO, instead of 0.5 wt% implied by the Na content, we obtain a reasonable stoichiometry whereby Si-5 + Al + Be ≈ 4 and Si-5 +

Na ≈ 0.24 ≈ Be, i.e., Na_x(Mg,Fe)₂(Al_{4-x-2y},Be_{x+y},Si_y)Si₅O₁₈, where x ≈ y ≈ 0.12, i.e., cordierite is calculated to contain 12% of the Na(Mg,Fe)₂Al₃BeSi₅O₁₈ end-member and 12% of the Mg₂[Al₂BeSi₆O₁₈] end-member.

Other minerals

Orthopyroxene included in surinamite contains 6.7 wt% Al₂O₃ (Table 5), similar to the amount in the intergrowths (up to 7.5 wt% Al₂O₃) but significantly less than the 8.1–9.7 wt% found in orthopyroxene porphyroblasts (Baba 1999). The X_{Mg} (= 0.78) of the orthopyroxene inclusion in surinamite is intermediate compared with the ranges obtained for orthopyroxene in intergrowths (X_{Mg} = 0.70–0.86) and porphyroblasts (0.75–0.86).

A sillimanite inclusion within surinamite differs from kyanite coexisting with surinamite not only in containing less Fe₂O₃, but also in being non-stoichiometric with an Al/Si ratio = 2.17 (Table 5). The non-stoichiometry is not due to included corundum, which has not been found in this rock, and differs from that reported for Be- and B-bearing pegmatite sillimanite (Grew et al. 1998), although similar to that expected in a solid solution toward mullite.

WHOLE-ROCK COMPOSITION

The specimen was crushed in a WC mill until the fragments reached 2 mm diameter and then reduced to powder in a quartz

TABLE 3. Representative analyses of sapphirine presumed to be beryllian in sample no. 96820-sp1

Anal. no. Index	C14-3 in Sur	A15-10 in Ky	B11-13 in Ky
Electron microprobe wt%			
SiO ₂	19.32	18.55	18.92
TiO ₂	0.08	0.11	0.01
Al ₂ O ₃	54.33	54.24	54.07
Cr ₂ O ₃	0.00	0.00	0.03
Fe ₂ O ₃	0.19	1.37	0.00
FeO	6.11	6.76	8.87
MnO	0.06	0.11	0.06
MgO	18.91	17.94	16.58
CaO	0.05	0.01	0.04
Na ₂ O	0.03	0.04	0.01
K ₂ O	0.00	0.00	0.00
Assumed BeO wt%			
BeO	1.25	1.25	1.25
Total	100.33	100.38	99.85
Structural formulae based on 28 cations			
O	40.000	40.000	40.060
Si	4.507	4.359	4.492
Ti	0.014	0.019	0.002
Al	14.938	15.018	15.129
Cr	0.000	0.000	0.006
Fe ³⁺	0.033	0.244	0.000
Fe ²⁺	1.192	1.326	1.760
Mn	0.012	0.021	0.011
Mg	6.577	6.285	5.870
Be	0.701	0.705	0.713
Na	0.014	0.018	0.006
Ca	0.012	0.003	0.011
K	0.000	0.000	0.000
X _{Mg}	0.847	0.826	0.769

Note: Fe₂O₃, FeO, Fe³⁺ and Fe²⁺ are calculated from charge balance. in Sur, inclusion within surinamite; in Ky, inclusion within kyanite; X_{Mg} = Mg/(Mg + Fe²⁺).

TABLE 4. Representative analyses of cordierite in sample no. 96820-sp1

Anal. no. Index	no.1-1/3 rep Sur	no.1-15 rep Sur	A19-25 rep int
Electron microprobe wt%			
SiO ₂	50.53	50.52	48.36
TiO ₂	0.02	0.00	0.17
Al ₂ O ₃	30.70	31.08	33.05
Cr ₂ O ₃	0.03	0.00	0.00
FeO*	2.18	2.03	3.14
MnO	0.05	0.02	0.06
MgO	11.61	11.65	11.23
CaO	0.04	0.04	0.00
Na ₂ O	0.54	0.56	0.07
K ₂ O	0.07	0.04	0.00
Assumed BeO wt%			
BeO	1.00	1.00	—
Total	96.76	96.94	96.08
Structural formulae based on 18 O atoms			
Si	5.122	5.106	4.977
Ti	0.001	0.000	0.013
Al	3.668	3.703	4.009
Cr	0.002	0.000	0.000
Fe	0.185	0.172	0.270
Mn	0.004	0.002	0.005
Mg	1.754	1.755	1.723
Be	0.244	0.243	—
Ca	0.004	0.004	0.000
Na	0.106	0.110	0.014
K	0.008	0.005	0.000
Total cations	11.099	11.100	11.012
X _{Mg}	0.905	0.911	0.864

Note: FeO*, total Fe as FeO; rep Sur, cordierite replacing surinamite; rep int, cordierite between orthopyroxene and kyanite; X_{Mg} = Mg/(Mg + Fe²⁺).

ball mill. Major constituents were analyzed by XRF and trace elements by various methods (Table 6).

The high-silica content and peraluminous composition (Baba 1998b, 1999, this paper) are consistent with a metasedimentary origin for the surinamite-bearing gneiss. Compared with other metasedimentary gneisses of the Leverburgh belt (Skinner 1970, in Garson and Livingstone 1973; Palmer 1971, in Fettes et al. 1992; Sheraton et al. 1973), the surinamite-bearing gneiss has a higher Mg-number (= 80) and marked depletion in Th, U, Y, and the rare earth elements. However, its high-Ba content and K/Rb ratio are characteristic of the Leverburgh belt gneisses. Sheraton (1980) inferred that the high Mg-numbers and trace-element depletions in metapelitic rocks from the Archean Napier Complex, Antarctica, are probably original features of their protoliths whereas high K/Rb ratios and depletion of Th and U are the result of ultrahigh temperature metamorphism of these rocks. Thus the distinctive trace-element signature of the surinamite-bearing rock is probably an original feature with the exception of the low contents of Rb, Cs, Li, Th, and U.

The Be content of the surinamite-bearing gneiss is near the upper limit of 0.5 to 10 ppm, which is the range reported for siliceous metamorphic rocks of different metamorphic grades (Hörmann 1969; Sighinolfi 1973; Lebedev and Nagaystev 1980; Bushlyakov and Grigor'yev 1988), including granulite-facies metapelites from Antarctica (except one rock at 23 ppm Be, Fig. 5). Thus, the presence of Be minerals is not an indication of unusual Be enrichment such as one might expect in a peg-

matite (cf., 44 ppm Be in a sheared pegmatite, Grew et al. 1995). Moreover, Be minerals have been reported in rocks containing even less Be: taaffeite in spinel-phlogopite schist from South Australia (5 ppm Be, Teale 1980) and beryllian sapphirine in quartzofeldspathic gneiss from the Napier Complex (5 ppm Be, no. 2045A, Grew 1981; Grew, Shearer, and Sheraton, unpublished data). The appearance of a discrete Be phase in rocks containing only a few ppm Be could result from the very low concentrations of that element accepted into the major constituents quartz, alkali feldspar, phlogopite, spinel, pyroxene, and kyanite. In contrast, at lower metamorphic grades where muscovite is stable, a discrete Be phase would not appear because all Be could be incorporated in muscovite, which is reported to contain up to 120 ppm Be (e.g., Grundmann and Morteani 1989). Similarly, a discrete Be phase would not be expected in cordierite-bearing metapelites unaffected by subsequent metamorphic events.

TABLE 5. Representative analyses of orthopyroxene inclusion and aluminosilicates in sample no. 96820-sp1

Anal. no. Index	B2-2 Opx(in Sur)	no.1-18 Sil(in Sur)	B11-7 Ky	no.1-24 Ky
Electron microprobe wt%				
SiO ₂	52.36	35.09	36.67	37.52
TiO ₂	0.28	0.00	0.15	0.03
Al ₂ O ₃	6.66	64.52	61.04	61.93
Cr ₂ O ₃	0.19	0.16	0.00	0.00
Fe ₂ O ₃	—	0.38	1.02	0.97
FeO*	13.50	—	—	—
MnO	0.54	0.09	0.03	0.00
MgO	26.83	0.03	0.01	0.00
CaO	0.19	0.03	0.01	0.01
Na ₂ O	0.11	0.00	0.11	0.00
K ₂ O	0.12	0.01	0.00	0.00
Total	100.84	100.31	99.04	100.46
Structural formulae				
O atoms	6	5	5	5
Si	1.855	0.949	1.005	1.012
Ti	0.007	0.000	0.003	0.001
Al	0.278	2.056	1.971	1.969
Cr	0.005	0.003	0.000	0.000
Fe ³⁺	0.004	0.009	0.023	0.022
Fe ²⁺	0.396	—	—	—
Mn	0.016	0.002	0.001	0.000
Mg	1.417	0.001	0.000	0.000
Ca	0.007	0.001	0.000	0.000
Na	0.008	0.000	0.006	0.000
K	0.005	0.000	0.000	0.000
Total cations	4.000	3.022	3.010	3.003
X _{Mg}	0.780	—	—	—

Note: FeO*, total Fe as FeO; in Sur, inclusion within surinamite. Fe³⁺ for orthopyroxene is estimated from charge balance.

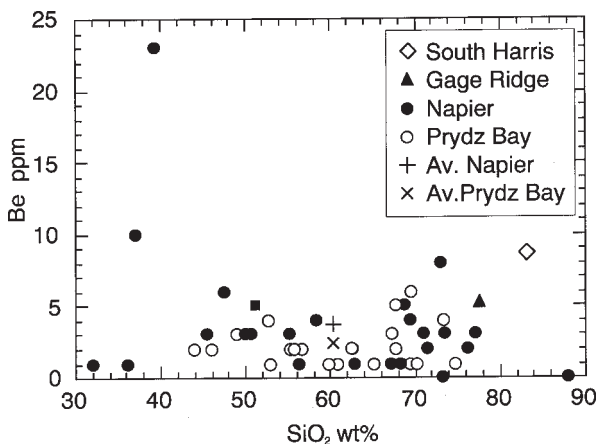


FIGURE 5. Beryllium content of specimen no. 96820-sp1 from South Harris (this paper) compared with Be contents of granulite-facies metapelites from the Napier Complex, including Gage Ridge (Sheraton 1980, 1985, and unpublished data) and Prydz Bay (Sheraton et al. 1984, and unpublished data), East Antarctica.

TABLE 6. Analyses of surinamite-bearing gneiss (no. 96820-sp1) from South Harris

wt%(XRF)		ppm	Method	ppm	Method
SiO ₂	83.31	Li 3.2*	ICP-MS	La 4.7	ICP-MS
TiO ₂	0.09	Be 8.7*	ICP-MS	Ce 7.7	ICP-MS
Al ₂ O ₃	9.22	B <20	ICP-AES	Pr 0.68	ICP-MS
Fe ₂ O ₃	0.76	F 130	ISE	Nd 2.4	ICP-MS
MnO	0.01	Cr 27	XRF	Sm 0.42	ICP-MS
MgO	1.51	Rb 58	XRF	Eu 0.61	ICP-MS
CaO	0.28	Sr 51	XRF	Gd 0.33	ICP-MS
Na ₂ O	0.70	Y 0.94	ICP-MS	Dy 0.19	ICP-MS
K ₂ O	3.46	Zr 91.7	ICP-MS	Er 0.12	ICP-MS
P ₂ O ₅	0.01	Nb 0.87	ICP-MS	Yb 0.15	ICP-MS
L.O.I.	0.01	Cs 0.43	ICP-MS	Lu 0.04	ICP-MS
Total	99.36	Ba 1664	XRF	Th 0.13	ICP-MS
		Hf 2.36	ICP-MS	U 0.11	ICP-MS
Mg'	0.80	Ta 0.17	ICP-MS		

Note: Analyses (except Li, Be and B) were performed at Australian National University (ANU). Abbreviations: L.O.I. = loss on ignition, XRF = X-ray fluorescence, ICP-MS = inductively coupled plasma mass spectrometry, ICP-AES = inductively coupled plasma atomic emission spectroscopy, ISE = ion selective electrode.

* Analyses by the Australian Geological Survey organization, with additional analyses by Analabs of Perth, Western Australia (Li 4.4 ppm, Be 9 ppm, B less than the 20 ppm detection limit).

A MODEL FOR SURINAMITE PARAGENESES AT SOUTH HARRIS AND OTHER LOCALITIES

To a first approximation, surinamite and associated minerals at South Harris can be represented by the model system $(\text{Mg,Fe,Zn})\text{O}-\text{BeO}-\text{Al}_2\text{O}_3-\text{SiO}_2$ where the relatively small amount of FeO and ZnO has been combined with MgO. Sillimanite and kyanite are present throughout the gneiss, and thus, we have projected the mineral compositions from Al_2SiO_5 onto the plane $(\text{Mg,Fe})\text{Al}_2\text{O}_4-\text{BeO}-\text{SiO}_2$ (Fig. 6). Surinamite formation and breakdown do not appear to involve either biotite or potassium feldspar and, consequently, K_2O has not been included in the model system. The Fe_2O_3 in sapphirine and Na_2O in cordierite have also been ignored in this model system.

Compositional relationships in Figure 6 can be used to infer reactions relating the succession of Be phases in the South Harris surinamite-bearing gneiss. Figure 7 is a P - T diagram based on a Schreinemaker net for the four critical ferromagnesian phases and quartz, which is a major constituent of this gneiss. We have combined FeO with MgO because MgO is dominant in all the ferromagnesian phases and fractionation of Mg and Fe^{2+} among them is relatively small, decreasing in X_{Mg} as follows: Be-Crd ($X_{\text{Mg}} = 0.90-0.91$) > Sur (0.86–0.88) > Opx included in Sur (0.78); Be-Spr (0.77–0.85) is variable. Strictly speaking, the reactions that are shown as univariant in Figure 7 are divariant; in addition, other divariant reactions, which in-

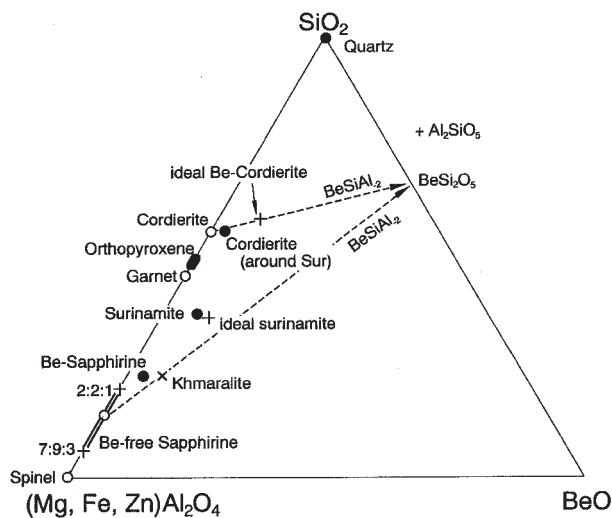
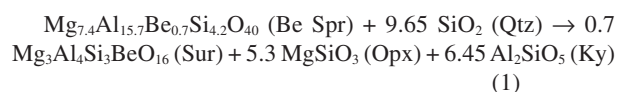


FIGURE 6. Mineral compositions projected through Al_2SiO_5 onto the plane Qtz (SiO_2)-Spl [$(\text{Mg,Fe,Zn})\text{Al}_2\text{O}_4$]-BeO (modified from Barbier et al. 1999). Filled circles and ellipse = measured compositions of minerals from South Harris; open circles = ideal compositions of Be-free phases; X = composition of khmaralite (Barbier et al. 1999); crosses = $\text{Mg}_2\text{Al}_2\text{BeSi}_6\text{O}_{18}$ cordierite (Hölscher and Schreyer 1989) and ideal surinamite (de Roever et al. 1981; Moore and Araki 1983). The dashed lines marked BeSiAl_2 are two of an array of lines converging on the point BeSi_2O_5 ; infinite amount of BeSiAl_2 substitution is required to reach this point along any one of these lines.

volve Fe-Mg fractionation, are possible. Nonetheless, divariance resulting from Mg-Fe fractionation plays a minor role compared with other compositional factors, and can be ignored given the other approximations in the present treatment.

The slopes of the reactions in the net have been constrained by the following considerations: (1) cordierite appears on the low-pressure side of all reactions involving it, and (2) surinamite appears on the high-pressure side of all reactions involving it except (Opx). Hölscher et al. (1986) argued that surinamite should appear on the high-pressure side of reactions because a higher proportion Al is incorporated in the denser form, i.e., octahedral coordination. Surinamite has a higher proportion of octahedral Al, 75%, than sapphirine (50%, Higgins and Ribbe 1979), khmaralite (60%, Barbier et al. 1999), orthopyroxene (50%), sillimanite (50%) and cordierite (0%). The Opx-absent reaction is shown as subvertical as surinamite and cordierite form together. The remaining question concerns the slopes of (Spr) and (Qtz). In the anhydrous, CO_2 -free and Na-free system, the slopes would more likely be positive because surinamite is more ordered than sapphirine and the cordierite solid solution, $\text{Mg}_2\text{Al}_4\text{Si}_5\text{O}_{18}-\text{Mg}_2\text{Al}_2\text{BeSi}_6\text{O}_{18}$, resulting in lower entropy as well as lower volume for the surinamite-bearing assemblages compared to the alternatives. Hölscher et al. (1986) reached a similar conclusion for the reaction surinamite = cordierite + sapphirine + enstatite + chrysoberyl. These positive slopes are appropriate for the South Harris rock because little Na_2O and H_2O were available and an estimated 50% of the Be was incorporated by BeSiAl_2 exchange in the cordierite. In contrast, beryllian cordierite at most other localities is sodian and hydrous and Be is incorporated almost exclusively by NaBeAl_1 exchange (e.g., Schreyer et al. 1979; Armbruster and Irouschek 1983). Breakdown of such cordierite to surinamite would be a dehydration, and the reactions (Qtz) and (Spr) could have negative slopes in presence of Na_2O and H_2O .

On the basis of recently discovered assemblages with sapphirine and orthopyroxene + Al_2SiO_5 at South Harris, the senior author proposed an anticlockwise P - T path for prograde metamorphism, which culminated at ultrahigh temperatures above 900 °C at 9–11 kbar pressures during the first stage (M1, Baba 1998a, 1998b, 1999). This stage was followed by recrystallization at more moderate temperatures of 850–900 °C at higher pressures of >12 kbar (M2). We infer that the rare sapphirine presently enclosed in Al_2SiO_5 (e.g., Baba 1999, Figs. 4c, 4d, and 4e) is a relic of the more abundant sapphirine that coexisted with matrix quartz and orthopyroxene during M1. In the transition from M1 to M2, when kyanite + orthopyroxene became stable, surinamite could have formed by the Crd-absent reaction (Fig. 7, calculated from simplified mineral compositions) with decreasing temperature and increasing pressure:



However, the Crd-absent reaction indicates formation of orthopyroxene and Al_2SiO_5 with surinamite, whereas textures in Figure 2a indicate that orthopyroxene and sillimanite are

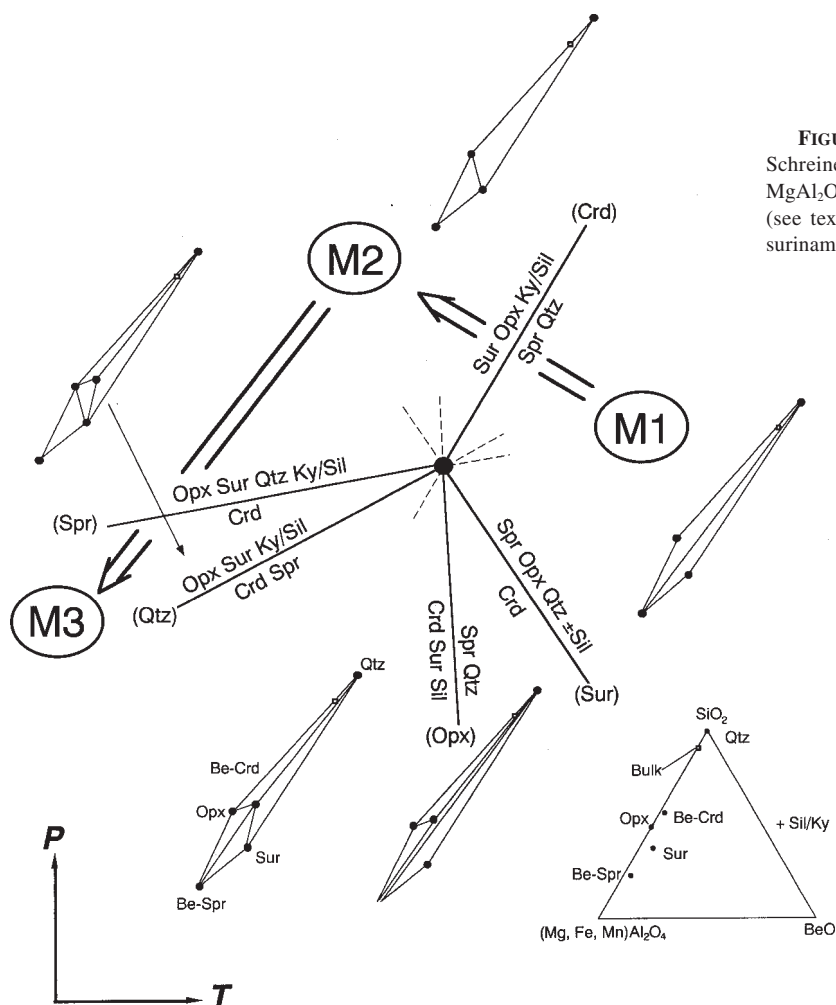
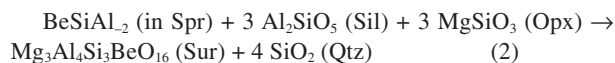


FIGURE 7. Pressure-temperature diagram based on a Schreinemaker net for phase relations in the system $\text{MgAl}_2\text{O}_4\text{-BeO-SiO}_2$ for assemblages containing Al_2SiO_5 (see text). Arrows indicate possible P - T path for the surinamite-bearing rock at South Harris.

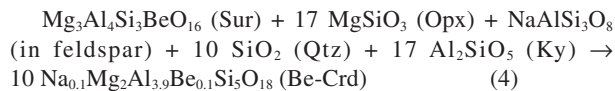
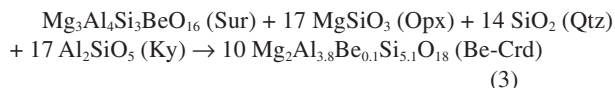
also relict phases. A reaction consistent with these textural relations is a continuous one whereby surinamite formed from the breakdown of the beryllium component of sapphirine:



Surinamite at South Harris most likely formed by both reactions, beginning with the continuous one and concluding with the Crd-absent one. This succession would explain the inclusions of Be-rich sapphirine, which were armored from further reaction by being enclosed in surinamite. As the continuous reaction progressed, sapphirine in the matrix became depleted in Be and, at some point, it was sufficiently depleted in Be that it became unstable with quartz and reacted with it by the Crd-absent reaction. In the end, no Be-poor sapphirine remained in the rock except as relics in surinamite. Sapphirine is rare now because most of it has reacted away to form surinamite, orthopyroxene, and Al_2SiO_5 .

Because compositional features of cordierite that surrounds surinamite suggest incorporation of Be by both the NaBeAl_1 and BeSiAl_2 exchanges, replacement of surinamite by cordi-

erite during M3 could have been by a combination of the following reactions, the first corresponding to (Spr) in Figure 7 and not involving Na_2O , the second involving Na_2O :



In summary, the formation of surinamite from beryllian sapphirine during M2 and its subsequent breakdown to beryllian cordierite during M3 can be explained by a counter-clockwise P - T loop in Figure 7.

Formation of surinamite at the other localities (Table 1) can be rationalized in terms of the model developed for South Harris. However, more compositional variables are involved, most importantly, FeO, Fe_2O_3 , ZnO, K_2O , and Na_2O . This variability results in the participation of additional phases, e.g., biotite, potassium feldspar, pyrope-almandine, spinel-hercynite,

and musgravite. De Roever et al. (1976) reported textural evidence at the Bakhuis Mountains, Surinam (type) locality for surinamite formation from breakdown of beryllian cordierite in mylonitic mesoperthitic gneiss with increasing pressure and temperature under conditions of the granulite facies. The reaction that de Roever et al. (1976) proposed for the Surinam occurrence, $\text{Crd} \rightarrow \text{Sur} + \text{Al}_2\text{SiO}_5 + \text{Qtz}$, is divariant in the model system $(\text{Mg,Fe})\text{Al}_2\text{O}_4\text{-BeO-SiO}_2$ and trivariant if either FeO or Fe_2O_3 is considered, both of which are present in significant amounts in surinamite. De Roever et al. (1976) contended that biotite, which is invariably associated with surinamite, formed subsequently to it. However, compositional data on the minerals associated with surinamite are needed to fix the surinamite-forming reaction better at the type locality. The surinamite-bearing rock from Chimwala, Zambia has many features in common with the rocks from the type locality (de Roever and Vrána 1985), but differs in the presence of garnet. Metamorphic grade is inferred to be transitional amphibolite-granulite facies, and surinamite formed with increasing pressure, but without a temperature increase. The reaction proposed by de Roever and Vrána (1985), $\text{Crd} + \text{Kfs} + \text{H}_2\text{O} \rightarrow \text{Bt} + \text{Ky} + \text{Sur} + \text{Qtz} + \text{Ab}$, is univariant in the model system $\text{K}_2\text{O-Na}_2\text{O-(Mg,Fe)Al}_2\text{O}_4\text{-BeO-SiO}_2$. However, neither the role of FeO, Fe_2O_3 , TiO_2 (in biotite), or CaO (in plagioclase), nor the participation of garnet and magnetite were considered. Again, compositional data are needed to assess the proposed reaction better.

Surinamite could have formed from cordierite with increasing pressure in the Strangways Range, Australia, but the reported textures are less definitive. Woodford and Wilson (1976) reported the breakdown of cordierite to orthopyroxene + sillimanite + quartz in the northeast Strangways Range, implying a pressure increase, and Goscombe (1992) proposed for this area a counter-clockwise P - T path with a pressure increase following a thermal maximum at 900–950 °C and 8–9 kbar.

Formation of surinamite in the granulite-facies meta-pegmatites of the Napier Complex, Antarctica, has been interpreted to be similar to its formation from cordierite in the Surinam and Zambia rocks although definitive evidence for a beryllian cordierite precursor is absent in the Napier pegmatites (de Roever and Vrána 1985; Grew 1998). In samples collected at “Christmas Point” in January, 1999, Grew et al. (1999, 2000) found textural evidence for the reactions $\text{Be-sapphirine/khmaralite} + \text{quartz} \rightarrow \text{garnet} + \text{sillimanite} + \text{surinamite}$ and $\text{Be-sapphirine/khmaralite} \rightarrow \text{musgravite} + \text{sillimanite} + \text{surinamite}$. There is no need to assume the presence of a cordierite precursor in the “Zircon Point,” “Christmas Point,” or Mount Pardoe pegmatites because surinamite more likely formed from a sapphirine-group mineral. These reactions are divariant in the model system $\text{FeAl}_2\text{O}_4\text{-MgAl}_2\text{O}_4\text{-BeO-SiO}_2$, but substantial Fe_2O_3 is present in sapphirine and surinamite and significant ZnO in musgravite (Grew 1981). The reactions for breakdown of beryllian sapphirine and khmaralite could be coeval with the reactions $\text{sapphirine} + \text{quartz} \rightarrow \text{garnet}$ and/or $\text{orthopyroxene} + \text{sillimanite}$ in host rocks to the beryllium pegmatites. These coronas have been interpreted to indicate an isobaric decrease in temperature consistent with a counter-clockwise P - T path for the Napier Complex (e.g., Sandiford and Wilson 1983; Motoyoshi and Hensen 1989; Harley 1998).

However, Grew et al. (1999, 2000) have proposed that the corona assemblages resulted from a superimposed metamorphic event sufficiently high in temperature and pressure to stabilize the sillimanite + orthopyroxene + quartz assemblage; that is, surinamite formed during a discrete high-temperature metamorphic event at relatively high pressure. Cordierite, kyanite, and andalusite are present in the beryllium pegmatites, but all three minerals are interpreted to postdate surinamite.

SUMMARY REMARKS

The following features characterize the eight known localities for surinamite:

(1) Surinamite is found in granulite- or upper-amphibolite-facies metapelites and metapegmatites with the assemblages sillimanite + potassium feldspar and kyanite + potassium feldspar in lieu of muscovite + quartz.

(2) Evidence for surinamite formation accompanied by anatexis is lacking, although surinamite occurs in rocks that had been melts, i.e., the Napier Complex pegmatites. Grew (1981) suggested a plutonic origin for surinamite in the Napier Complex pegmatites, but later re-interpreted the textures as metamorphic (Grew 1998; Grew et al. 1999, 2000), and thus there is no evidence for a plutonic surinamite reported to date.

(3) Surinamite-bearing rocks are typically polymetamorphic; in most cases, there is evidence for a pre-existing phase enriched in beryllium. Mylonitic textures are characteristic of several examples, notably, South Harris and Bakhuis Mountains; there is evidence for granulation in the pegmatite at “Christmas Point.” In all cases, surinamite formed with an increase in pressure and/or decrease in temperature or simple decrease in temperature on an anti-clockwise P - T path; no examples are known of surinamite forming as pressure decreased.

(4) Surinamite is not restricted to rocks enriched in Be, but its formation depends on a mechanism for concentrating disseminated beryllium. This mechanism appears to be formation of a mineral such as cordierite or sapphirine that can scavenge Be from a large mass of rock and becomes the locus of surinamite crystallization during a succeeding metamorphic event. Conditions during this event must be such that Be is not newly dispersed. Low water activities probably restrict its mobility. That beryllium is not dispersed anew is evident in the heterogeneous cordierite compositions in the South Harris rock; cordierite formed from surinamite appears to be beryllian, whereas cordierite formed between orthopyroxene and kyanite in the same specimen shows no compositional anomalies indicative of beryllium incorporation.

ACKNOWLEDGMENTS

We are grateful to M. Arima for his kind arrangement in starting this work at the International Symposium “Origin and Evolution of Continents” held in Tokyo in October, 1997. S.B. thanks M. Komatsu and A.J. Barber for support during fieldwork at Harris in 1995 and 1996 and for permission to carry out EPMA analyses at Ehime University. S.B. also thanks “Fukada Geological Institute” and “Japan Society for the Promotion of Science” for their financial support. E.S.G.’s research was supported by NSF grant OPP-9813569 to the University of Maine. The ion microprobe data presented here were measured at the University of New Mexico/Sandia National Laboratories SIMS facility, a national user facility supported in part by NSF grant EAR97-06054. U. Senff and S. Eggins (ANU), and B. Cruikshank (AGSO) are thanked for the whole-rock analyses, and J. Barbier for his unpublished data on surinamite structure. We thank S.L. Harley and D. Henry for their detailed and thoughtful reviews of an earlier draft.

REFERENCES CITED

- Armbruster, T. (1986) The role of Na in the structure of low cordierite: single crystal X-ray study. *American Mineralogist*, 71, 746-757.
- Armbruster, T. and Irouschek, A. (1983): Cordierites from the Lepontine Alps: Na + Be → Al substitution, gas content, cell parameters, and optics. *Contributions to Mineralogy and Petrology*, 82, 389-396.
- Baba, S. (1998a) Proterozoic anticlockwise *P-T* path of the Lewisian Complex of South Harris, Outer Hebrides, NW Scotland. *Journal of Metamorphic Geology*, 16, 819-841.
- (1998b) Ultra-high temperature metamorphism in the Lewisian Complex, South Harris, NW Scotland. In Y. Motoyoshi, and K. Shiraishi, Eds., *Origin and Evolution of Continents*, Memoirs of National Institute of Polar Research Special Issue, 53, 93-108.
- (1999) Sapphirine-bearing orthopyroxene-kyanite/sillimanite granulites from South Harris, NW Scotland: evidence for Proterozoic UHT metamorphism in the Lewisian. *Contributions Mineralogy and Petrology*, 136, 33-47.
- Barbier, J., Grew, E.S., Moore, P.B., and Su, S.-C. (1999) Khmaralite, a new beryllian mineral related to sapphirine: an example of a superstructure resulting from partial ordering of Be, Al and Si on tetrahedral sites. *American Mineralogist*, 84, 1650-1660.
- Bushlyakov, I.N. and Grigor'ev, N.A. (1989) Beryllium in Ural metamorphites. *Geochemistry International*, 26(4), 57-61.
- Černý, P. and Povondra, P. (1966) Beryllian cordierite from Věžná: (Na,K) + Be = Al. *Neues Jahrbuch für Mineralogie Monatshefte*, 36-44.
- Cliff, R.A., Gray, C.M., and Huhma, H. (1983) Sm-Nd Isotopic Study of the South Harris Igneous Complex, the Outer Hebrides. *Contributions Mineralogy and Petrology*, 82, 91-98.
- de Roever, E.W.F. (1973) Preliminary note on coexisting sapphirine and quartz in a mesoperthite gneiss from Bakhuis Mountains (Surinam). *Geologische Mijnbouwkundige Dienst Suriname Mededeling*, 22, 67-70.
- de Roever, E.W.F. and Vrána, S. (1985) Surinamite in pseudomorphs after cordierite in polymetamorphic granulites from Zambia. *American Mineralogist*, 70, 710-713.
- de Roever, E.W.F., Kieft, C., Murray, E., Klein, E., and Drucker, W.H. (1976) Surinamite, a new Mg-Al silicate from the Bakhuis Mountains, western Surinam. I. Description, occurrence, and conditions of formation. *American Mineralogist*, 61, 193-199.
- de Roever, E.W.F., Lattard, D., and Schreyer, W. (1981) Surinamite: A beryllium-bearing mineral. *Contributions to Mineralogy and Petrology*, 76, 472-473.
- Fettes, D.J., Mendum, J.R., Smith, D.I., and Watson, J.V. (1992) *Geology of Outer Hebrides*. 175 p. British Geological Survey, London, U.K.
- Garson, M.S. and Livingstone, A. (1973) Is the South Harris complex in north Scotland a Precambrian overthrust slice of oceanic crust and island arc? *Nature Physical Science*, 243, 74-76.
- Goscombe, B. (1992) Silica-undersaturated sapphirine, spinel and kornorupine granulite facies rocks, NE Strangways Range, Central Australia. *Journal of Metamorphic Geology*, 10, 181-201.
- Grew, E.S. (1981) Surinamite, taaffeite, and beryllian sapphirine from pegmatites in granulite-facies rocks of Casey Bay, Enderby Land, Antarctica. *American Mineralogist*, 66, 1022-1033.
- (1998) Boron and beryllium minerals in granulite-facies pegmatites and implications of beryllium pegmatites for the origin and evolution of the Archaean Napier Complex of East Antarctica. In Y. Motoyoshi, and K. Shiraishi, Eds., *Origin and Evolution of Continents*, Memoirs of National Institute of Polar Research Special Issue, 53, 74-92.
- Grew, E.S., Hiroi, Y., Motoyoshi, Y., Kondo, Y., Jayatileke, S.J.M., and Marquez, N. (1995) Iron-rich kornorupine in sheared pegmatite from Wannu Complex, at Homagama, Sri Lanka. *European Journal of Mineralogy*, 7, 623-636.
- Grew, E.S., Yates, M. G., Huijsmans, J.P.P., McGee, J.J., Shearer, C.K., Wiedenbeck, M., and Rouse, R.C. (1998) Werdingite, a borosilicate new to granitic pegmatites. *Canadian Mineralogist*, 36, 399-414.
- Grew, E.S., Barbier, J., Shearer, C.K., Sheraton, J.W., and Shiraishi, K. (1999) Granulite-facies Beryllium Pegmatite in the Napier Complex at Khmara and Amundsen Bays, western Enderby Land, East Antarctica. The 19th Symposium on Antarctic Geosciences, Program and Abstracts, National Institute of Polar Research, Tokyo, Japan, October 14-15, 1999.
- Grew, E.S., Yates, M.G., Barbier, J., Shearer, C.K., Sheraton, J.W., Shiraishi, K., and Motoyoshi, Y. (2000) Granulite-facies beryllium pegmatites in the Napier Complex in Khmara and Amundsen Bays, western Enderby Land, East Antarctica. *Polar Geoscience*, 13, in press.
- Grundmann, G. and Morteani, G. (1989) Emerald mineralization during regional metamorphism: The Habachtal (Austria) and Leydsdorp (Transvaal, South Africa) deposits. *Economic Geology*, 84, 1835-1849.
- Harley, S. L. (1998) On the occurrence and characterization of ultrahigh-temperature crustal metamorphism. In P.J. Treloar and P.J. O'Brien, Eds., *What Drives Metamorphism and Metamorphic Reactions?*, 138, 81-107. Special Publications, Geological Society, London.
- Higgins, J.B. and Ribbe, P.H. (1979) Sapphirine II: A neutron and X-ray diffraction study of (Mg-Al)^{VI} and (Al-Si)^{IV} ordering in monoclinic sapphirine. *Contributions to Mineralogy and Petrology*, 68, 357-368.
- Hölscher, A. and Schreyer, W. (1989) A new synthetic hexagonal BeMg-cordierite, Mg₂[Al₂BeSi₆O₁₈], and its relationship to Mg-cordierite. *European Journal of Mineralogy*, 4, 193-207.
- Hölscher, A., Schreyer, W., and Lattard, D. (1986) High-pressure, high-temperature stability of surinamite in the system MgO-BeO-Al₂O₃-SiO₂-H₂O. *Contributions to Mineralogy and Petrology*, 92, 113-127.
- Hörmann, P.K. (1969) *Handbook of Geochemistry, Beryllium B-O*. Springer-Verlag, Berlin-Heidelberg.
- Lebedev, V.I. and Nagaytsev, Yu.V. (1980) Minor elements in metamorphic rocks as an ore-material source for certain deposits. *Geochemistry International*, 17(6), 31-39.
- Moore, P.B. and Araki, T. (1983) Surinamite, *ca.* Mg₂Al₂Si₆BeO₁₆: its crystal structure and relation to sapphirine, *ca.* Mg_{2.8}Al_{1.2}Si₆O₁₆. *American Mineralogist*, 68, 804-810.
- Motoyoshi, Y. and Hensen, B.J. (1989) Sapphirine-quartz-orthopyroxene symplectites after cordierite in the Archaean Napier Complex, Antarctica: evidence for a counter clockwise *P-T* path? *European Journal of Mineralogy*, 1, 467-471.
- Palmer, K.F. (1971) A comparative study of two Pre-Cambrian gneiss areas—the Suportoq region, East Greenland, and South Harris, Outer Hebrides—and their bearing on Precambrian crustal evolution. Ph.D. thesis, University of Birmingham, Birmingham, U.K.
- Ramesh Kumar, P.V., Raju, K.K.V.S., and Ganga Rao, B.S. (1995) Surinamite (Be, B, Ga) from cordierite gneisses of eastern Ghat mobile belt, India. *Current Science*, 69(6), 763-767.
- Sandiford, M. and Wilson, C.J.L. (1983) The geology of the Fyfe Hills-Khmara Bay region, Enderby Land. In R.L. Oliver, P.R. James, and J.B. Jago, Eds., *Antarctic Earth Science*, p. 16-19. Australian Academy of Science, Canberra.
- Schreyer, W., Gordillo, C.E., and Werding, G. (1979) A new sodian-beryllian cordierite from Soto, Argentina, and the relationship between distortion index, Be content, and state of hydration. *Contributions to Mineralogy and Petrology*, 70, 421-426.
- Sheraton, J.W. (1980) Geochemistry of Precambrian metapelites from East Antarctica: secular and metamorphic variations. *BMR Journal of Australian Geology and Geophysics*, 5, 279-288.
- (1985) Chemical analyses of rocks from East Antarctica. *Australia Bureau of Mineral Resources, Geology and Geophysics Record* 1985/12, 124 p.
- Sheraton, J.W., Skinner, A.C., and Tarney, J. (1973) The geochemistry of the Scourian gneisses of Assynt district. In R.G. Park and J. Tarney, Eds., *The early Precambrian of Scotland and related rocks of Greenland*. p. 13-30. University of Keele, Keele.
- Sheraton, J.W., Black, L.P., and McCulloch, M.T. (1984) Regional geochemical and isotopic characteristics of high-grade metamorphics of the Prydz Bay area: the extent of Proterozoic reworking of Archaean continental crust in East Antarctica. *Precambrian Research*, 26, 169-198.
- Sighinolfi, G.P. (1973) Beryllium in deep-seated crustal rocks. *Geochimica et Cosmochimica Acta*, 37, 702-706.
- Skinner, A.C. (1970) Geochemical studies of the Lewisian of NW Scotland and comparable rocks in E Greenland. Ph.D. thesis, University of Birmingham, Birmingham, U.K.
- Teale, G.S. (1980) The occurrence of högbomite and taaffeite in a spinel-phlogopite schist from the Mount Painter Province of South Australia. *Mineralogical Magazine*, 43, 575-577.
- Vavrdra, I. and Vrána, S. (1972) Sillimanite, kyanite and andalusite in the granulite facies rocks of the basement complex, Chipata district. *Records of the Geological Survey Zambia*, 12, 69-80.
- Wood, B.J. (1975) The influence of pressure, temperature and bulk composition on the appearance of garnet in orthogneisses—an example from South Harris, Scotland. *Earth Planetary Sciences Letters*, 26, 299-311.
- (1977) The activities of components in clinopyroxene and garnet solid solutions and their application to rock. *Philosophical Transactions of the Royal Society of London*, 286, 331-342.
- Woodford, P.J. and Wilson, A.F. (1976) Sapphirine, högbomite, kornorupine, and surinamite from aluminous granulites, north-eastern Strangways Range, central Australia. *Neues Jahrbuch für Mineralogie Monatshefte*, 15-35.

MANUSCRIPT RECEIVED AUGUST 30, 1999

MANUSCRIPT ACCEPTED JUNE 15, 2000

PAPER HANDLED BY JOHN C. SCHUMACHER